Journal of Photochemistry and Photobiology A: Chemistry 231 (2012) 45–50

Contents lists available at SciVerse ScienceDirect

Journal of Photochemistry and Photobiology A: Chemistry

journal homepage: www.elsevier.com/locate/jphotochem

Photooxidation of $CF_3CF_2C(O)Cl$ in the presence of NO_2. Synthesis and characterization of pentafluoroethyl peroxynitrate, $CF_3CF_2OONO_2$

Adriana G. Bossolasco, Fabio E. Malanca*, Gustavo A. Argüello

INFIQC (CONICET), Departamento de Fisicoquímica, Facultad de Ciencias Químicas, Universidad Nacional de Córdoba, Córdoba, Argentina

ARTICLE INFO

Article history:
Received 27 July 2011
Received in revised form 11 January 2012
Accepted 15 January 2012
Available online 23 January 2012

Keywords:
Peroxynitrates
Fluorinated peroxynitrates
$CF_3CF_2OONO_2$
$CF_3CF_2C(O)Cl$
Photooxidation

ABSTRACT

The photolysis of $CF_3CF_2C(O)Cl$ in the presence of NO_2 and O_2 at 254 nm leads initially to the formation of $CF_3CF_2OONO_2$, CF_2O, and CO as the main carbonaceous products. The NO_2 concentration governs the identity of the products. As photolysis continues the NO_2 concentration gradually decreases until new channels open up and the mechanism leads to the formation of CF_2O, CO_2 and $CF_3OC(O)OONO_2$.

In addition to the study of the mechanism, we present in this paper some characteristics of the pentafluoroethyl peroxynitrate, $CF_3CF_2OONO_2$ such as the infrared spectrum with the associated absorption cross-sections for the main peaks and kinetic parameters for its thermal decomposition at total pressures of 9.0 and 250 mbar ($E_a = 87.7$ kJ/mol, $A = 3.8 \times 10^{13}$; and $E_a = 96.7$ kJ/mol, $A = 2.37 \times 10^{15}$, respectively) which show that they are dependent both on the temperature and on the total pressure.

1. Introduction

The atmospheric degradation of chlorofluorocarbons (CFCs) has received continued attention in the last decades because they are chemically inert in the troposphere, and can be transported to the stratosphere where they are photolyzed producing Cl atoms, which contribute to the ozone layer depletion [1,2].

Hydrochlorofluorocarbons (HCFCs) and hydrofluorocarbons (HFCs) have gained widespread use as CFCs substitutes since they can react with the hydroxyl radical ($HO^\bullet$), and consequently their atmospheric lifetimes are shorter than those corresponding to CFCs [1]. It is therefore necessary to understand not only the reaction mechanisms that the atmospheric degradation of HCFCs and HFCs themselves involve, but also the subsequent degradation mechanisms corresponding to the products formed.

Perhalogenated carbonyl compounds can be formed in the tropospheric degradation of HCFCs and HFCs. Perfluoroacetyl chloride ($CF_3C(O)Cl$), perfluoroacetyl fluoride ($CF_3C(O)F$), and perfluoropropionyl chloride ($CF_3CF_2C(O)Cl$) are formed in the tropospheric degradation of HCFC-124 (CF_3CHFCl), HCFC-141b (CF_3CHCl_2) and HCFC-225ca ($CF_3CF_2CHCl_2$) respectively [3,4]. In particular, Tuazón and Atkinson studied the photooxidation of $CF_3CF_2CHCl_2$ and determined that $CF_3CF_2C(O)Cl$ is produced in 100% yield [4].

The photochemistry of perhalogenated carbonyl compounds has been studied under different conditions (as pure compounds or in the presence of either O_2 or O_2/CO) by several authors [5–8]. The photochemical rupture of $CF_3CF_2C(O)Cl$ at 254 nm was studied by Cariati et al. [7] and Malanca et al. [5], who determined the primary path for the photolytic rupture of the molecule,

$$CF_3CF_2C(O)Cl \rightarrow CF_3CF_2^\bullet + CO + Cl^\bullet \quad (1)$$

the quantum yield ($\phi = 1.01 \pm 0.06$), and the reaction mechanism in the presence of O_2 and CO.

In this paper we have studied the photolysis of $CF_3CF_2C(O)Cl$ in the presence of NO_2 and O_2, in order to determine the reaction mechanism and the peroxynitrates ($ROONO_2$) that could possibly be formed during the atmospheric degradation of this compound. We have also compared the physicochemical properties of $CF_3CF_2OONO_2$ with other known peroxynitrates (e.g. trifluoromethyl (CF_3OONO_2), trifluoroacetyl ($CF_3C(O)OONO_2$), and trifluoromethoxycarbonyl ($CF_3OC(O)OONO_2$) peroxynitrates.

2. Experimental

2.1. Photolysis of $CF_3CF_2C(O)Cl$ in the presence of O_2/NO_2. Synthesis of $CF_3CF_2OONO_2$

Photolysis of $CF_3CF_2C(O)Cl$ was performed in a standard glass infrared cell (23.0 cm path length), located in the optical path of an IFS66v FTIR spectrophotometer which allowed us to monitor the appearance of products and the disappearance of reactants as a function of time. The reaction mechanism proposed was corroborated by comparing the experimental temporal evolution of reactants and products with a kinetic model (KINTECUS) [9].

* Corresponding author. Tel.: +54 351 433 4169; fax: +54 351 433 4188.
E-mail address: fmalanca@fcq.unc.edu.ar (F.E. Malanca).

1010-6030/$ – see front matter © 2012 Elsevier B.V. All rights reserved.
doi:10.1016/j.jphotochem.2012.01.009

The photolysis was carried out at room (22 °C) and at low (7 °C) temperatures as a means to test whether a decrease in temperature leads to higher $CF_3CF_2OONO_2$ concentrations, in order to select the adequate experimental conditions for the future synthesis of $CF_3CF_2OONO_2$. As it is known, low temperatures prevent thermal decomposition of peroxynitrates, and therefore the synthesized amount of $CF_3CF_2OONO_2$ increases.

The synthesis of $CF_3CF_2OONO_2$ was conducted using a 10 L glass flask and keeping temperature at 7 °C. Typical pressures of $CF_3CF_2C(O)Cl$, NO_2, and O_2 used were: 2.0, 0.5 and 1000 mbar, respectively.

The progress was monitored every 30 min through infrared spectroscopy (transferring approximately 1% of the mixture to the IR cell each time) and photolysis was stopped when NO_2 concentration had decreased to one third of its initial value (approximately 2.5 h of irradiation). The resultant mixture was collected by slowly passing it through three traps kept at −186 °C in order to remove excess O_2 and CO formed. It was then dynamically distilled between −85 and −120 °C to remove CF_2O and CO_2. Suction of the vacuum pump was stopped and the bath at −85 °C was allowed to slowly warm up to remove the unreacted $CF_3CF_2C(O)Cl$. The remnant fraction contained only $CF_3CF_2OONO_2$.

2.2. Infrared absorption cross-sections

The gas phase infrared spectrum was recorded at room temperature with a resolution of 2 cm^{-1} in the range of 4000–400 cm^{-1}, and the absorption cross-sections were calculated according to the following equation:

$$\sigma(cm^2\ mol^{-1}) = 31.79 \times 10^{-20}(mbar\ cm^3\ mol^{-1}\ K^{-1}) \times T \times A \times (p \times d)^{-1} \quad (2)$$

where T is the temperature (K), A is the absorbance, p is the pressure (mbar) and d is the optical path (cm). The pressures of $CF_3CF_2OONO_2$ ranged from 0.7 to 1.5 mbar.

2.3. Thermal decomposition

The rate constant for the thermal decomposition of $CF_3CF_2OONO_2$ was studied at room temperature as a function of total pressure, which ranged from 4.7 to 250 mbar. Typical runs were 1.0–2.0 mbar of peroxynitrate, 2.0 mbar of NO (that assures the capture of every radical formed), and N_2 up to the total pressure. The temporal variation of the infrared band at 1764 cm^{-1} was used to collect the data.

The temperatures ranged between 279 and 290 K. The data at each temperature and pressure were analyzed according to a first-order rate law. For each temperature, the decay was fitted by a linear regression and the value associated with the rate constant, together with its statistical uncertainty (as vertical bar), was plotted in the Arrhenius form.

3. Results and discussion

3.1. Photolysis of $CF_3CF_2C(O)Cl$ in the presence of O_2/NO_2

The spectra obtained for $CF_3CF_2C(O)Cl/NO_2/O_2$ mixtures at different irradiation times are shown in Fig. 1. As it can be seen, at 30 min the photolysis leads to the formation of $CF_3CF_2OONO_2$, CF_2O and CO_2 as the main carbonaceous products, while at 70 min the main carbonaceous products are CF_2O, $CF_3OC(O)OONO_2$, and CO_2. Carbon monoxide is a minor product at both photolysis times.

The complete reaction mechanism was postulated according to the products observed and the kinetic analysis performed, as it will be discussed below. Scheme 1 provides a simplified version

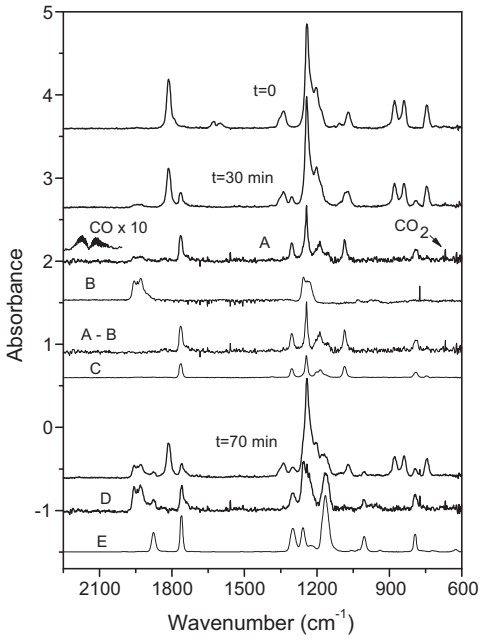

Fig. 1. Photooxidation of $CF_3CF_2C(O)Cl$ in the presence of NO_2. From top to bottom, the traces correspond to: t = 0 min; t = 30 min of photolysis; products at 30 min "A"; CF_2O reference spectrum "B"; subtraction of trace "A" minus "B"; $CF_3CF_2OONO_2$ reference spectrum "C"; t = 70 min of photolysis; products at 70 min "D"; $CF_3OC(O)OONO_2$ reference spectrum "E".

of the reaction mechanism to quickly visualize the main reactions leading to the more abundant fluorinated products. In general terms, the mechanism could be described as the photolysis of $CF_3CF_2C(O)Cl$ yielding the formation of perfluorinated radicals (R•), carbon monoxide, and chlorine atoms followed by the typical series of reactions occurring when O_2 and NO_2 are present, i.e. the reaction with O_2 to give the corresponding peroxy radicals (ROO•), which subsequently lead to either oxy radicals (RO•) or the corresponding peroxynitrate.

Two peroxynitrates can be observed in our system: $CF_3CF_2OONO_2$ and $CF_3OC(O)OONO_2$, whose formation depends on NO_2 concentration; when it is high, $CF_3CF_2OONO_2$ is formed since

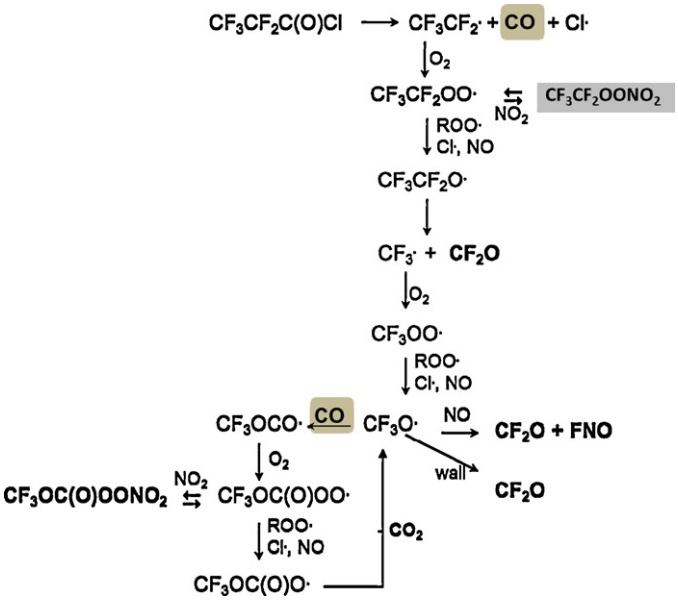

Scheme 1. Mechanism of photooxidation of $CF_3CF_2C(O)Cl$.

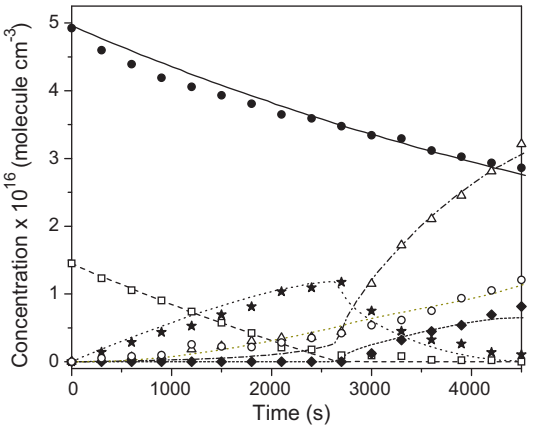

Fig. 2. Temporal variation of reactants and products in the photolysis of a mixture containing $CF_3CF_2C(O)Cl$, NO_2 and O_2. Symbols correspond to: $CF_3CF_2C(O)Cl$ (●), NO_2 (□), $CF_3CF_2OONO_2$ (☆), CF_2O (△), $CF_3OC(O)OONO_2$ (⧫) and CO_2 (○). Lines represent the best fit given by the KINTECUS model.

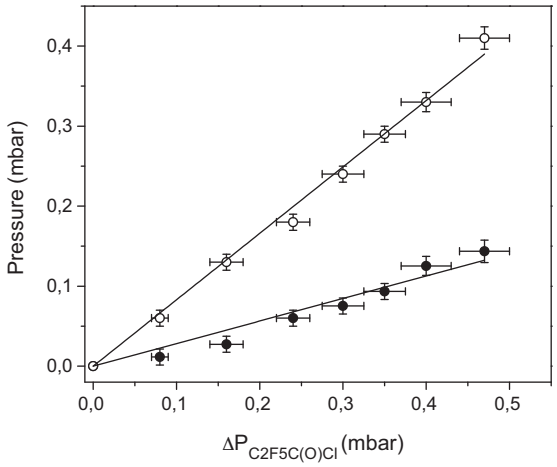

Fig. 3. Fluorinated products (○ CF_2O; ● $CF_3CF_2OONO_2$) as a function of the $CF_3CF_2C(O)Cl$ consumed in the presence of high NO_2 concentrations.

$CF_3CF_2OO^•$ are efficiently trapped by nitrogen dioxide. On the other hand, when NO_2 concentration is low, the formation of CF_2O and $CF_3OC(O)OONO_2$ prevails. The formation of this *peroxyacyl* nitrate is a consequence of both the increase in CO concentration due to the progress of the photolysis and the slow disappearance of $CF_3CF_2OONO_2$.

The temporal variations of reactants and main products are presented in Fig. 2, and the complete set of reactions used to model the system is shown in Table 1. The listed rate constant values were either obtained from the literature, determined experimentally in this work, or assumed to be similar to those of other reactions when kinetic data were not available. It is important to notice that Table 1 shows all those reactions considered in the model for which a good fit to the experimental data was obtained.

Fig. 2 shows that at the early stages of the reaction, when the NO_2 concentration is high, $CF_3CF_2OONO_2$ concentration increases, while it decreases as NO_2 concentration does so. Once the NO_2 concentration has decreased to around 85% of its initial value, the reactions of $CF_3CF_2OO^•$ radicals with the other species present in the system (NO, Cl, $ROO^•$; R = CF_3CF_2, CF_3, $CF_3OC(O)$) start to take place, the rate of formation of $CF_3CF_2OONO_2$ decreases and its thermal decomposition begins to prevail. The rupture of this peroxynitrate leads to the formation of CF_2O and CF_3 radicals, that are converted to CF_3O radicals as consequence of subsequent reactions. At about 2700 s-photolysis time, two channels are available for CF_3O radicals: that contributing to the formation of CF_2O, and the important one to this manuscript that is the reaction with CO (present in the system as a consequence of the progress of $CF_3CF_2C(O)Cl$ photolysis) that leads finally to $CF_3OC(O)OONO_2$ formation (Scheme 1). Both together provide $CF_3OC(O)OONO_2$ and an increase in CF_2O concentration, in agreement with the experimental data.

The rate constant for the photolysis of $CF_3CF_2C(O)Cl$ ($k = 1.30 \times 10^{-4}\,s^{-1}$) was experimentally obtained following the disappearance of its peak at 1814 cm^{-1} as a function of time. The values of the rate constants for the reactions leading to the formation of the observed peroxynitrates (rows 3 and 17) were adjusted to the kinetic model, using as starting points the values informed by Giessing et al. [10] and Wallington et al. [11], respectively. Some other reactions have also been included in the mechanism due to the presence of the chlorinated radicals Cl, $ClCO^•$, $ClC(O)O_2^•$ and $ClC(O)O^•$ (rows 31–35) needed to fit the CO_2 concentration. The photolysis of NO_2 (row 36) has been also included because this compound absorbs at the photolysis wavelength ($\sigma = 1.09 \times 10^{-20}\,cm^2\,molecule^{-1}$) [12]. Nitrosyl fluoride (FNO) formation – proposed in row 14 – was not observed in the infrared spectra shown in Fig. 1, probably as a consequence of either its small infrared absorption cross-section or the fact that it reacts at the walls of the infrared cell, in agreement with observations reported by Manetti et al. [13].

A sensitivity analysis was carried out to check the relative importance of the set of reactions that are related with the production of the main fluorinated products ($CF_3CF_2OONO_2$, $CF_3OC(O)OONO_2$ and CF_2O), used in the kinetic model. The analysis starts with the reactions that have a continued contribution both at short and long times, and then, we analyze the contribution to either one of these time periods. Only reactions with significant relative sensitivity coefficients will be discussed.

The analysis of the sensitivity coefficients for the mechanism listed in Table 1 reveals that the rate constants for reactions in rows 1, 3 and 4 are the most important ones to achieve good fits of the experimental data. It is important to note that reactions 1 and 4 were both measured in this work and their rate constant values are within the expected ones for similar systems [10]. On the other hand, reaction in row 6 (which provides the unstable oxy radical $CF_3CF_2O^•$) has a significant coefficient for the formation of CF_2O and acts as a sink for $CF_3CF_2OONO_2$ only at short times, while contributing significantly to the formation of $CF_3OC(O)OONO_2$ at long times.

Reactions in rows 17 and 31, affecting the concentration of $CF_3OC(O)OONO_2$, are relevant at long times. This is in agreement with the fact that reaction in row 17 leads to the formation of peroxynitrate, while reaction in row 31 consumes CO and could prevent its formation.

Though the sensitivity analysis reveals that only a few coefficients have significant values; all the reactions considered here are necessary to get a good fit of the time progression of the system.

Fig. 3 shows the fluorinated products formed as a function of the pressure of the $CF_3CF_2C(O)Cl$ consumed, at high NO_2 concentrations (short photolysis times). The slopes of the straight lines obtained from linear least-squares fits give the relative molar yields for $CF_3CF_2OONO_2$ (83 ± 1)%, and CF_2O (28 ± 2)%. Quoted errors correspond to one standard deviation from the regression analysis. Within the experimental uncertainties, the observed formation of CF_2O, and $CF_3CF_2OONO_2$ accounts for (97 ± 5)% of the total loss of $CF_3CF_2C(O)Cl$ (note that one CF_3CF_2 fragment leads to the formation of one pentafluoroethyl peroxy nitrate molecule or two carbonyl fluoride molecules, so that the fluorocarbon balance is $\Delta[CF_3CF_2C(O)Cl] = [CF_3CF_2OONO_2] + 1/2\,[CF_2O]$).

Table 1
Rate constants used in the kinetic model (KINTECUS).

	Reaction	k[a]	Reference
1	$CF_3CF_2C(O)Cl \rightarrow CF_3CF_2 + CO + Cl$	1.30×10^{-4}	This work (see text)
2	$CF_3CF_2 + O_2 \rightarrow CF_3CF_2OO$	1.10×10^{-11}	[22]
3	$CF_3CF_2OO + NO_2 \rightarrow CF_3CF_2OONO_2$	7.00×10^{-12}	[b]
4	$CF_3CF_2OONO_2 \rightarrow CF_3CF_2OO + NO_2$	2.60×10^{-2}	This work
5	$CF_3CF_2OO + NO \rightarrow CF_3CF_2O + NO_2$	1.10×10^{-11}	[23]
6	$CF_3CF_2OO + Cl \rightarrow CF_3CF_2O + ClO$	4.20×10^{-11}	Assumed similar to react 12
7	$2CF_3CF_2OO \rightarrow 2CF_3CF_2O + O_2$	2.26×10^{-12}	[24]
8	$CF_3CF_2O \rightarrow CF_3 + CF_2O$	2.18×10^{7}	[25]
9	$CF_3 + O_2 \rightarrow CF_3OO$	9.00×10^{-12}	[26]
10	$CF_3OO + NO \rightarrow CF_3O + NO_2$	1.60×10^{-11}	[19]
11	$2CF_3OO \rightarrow 2CF_3O + O_2$	2.26×10^{-12}	[27]
12	$CF_3OO + Cl \rightarrow ClO + CF_3O$	4.20×10^{-11}	[24]
13	$CF_3O + NO_2 \rightarrow CF_3ONO_2$	1.65×10^{-11}	[28]
14	$CF_3O + NO \rightarrow CF_2O + FNO$	5.34×10^{-11}	[29]
15	$CF_3O + CO \rightarrow CF_3OCO$	5.00×10^{-13}	[30]
16	$CF_3OCO + O_2 \rightarrow CF_3OC(O)OO$	7.31×10^{-13}	[c]
17	$CF_3OC(O)OO + NO_2 \rightarrow CF_3OC(O)OONO_2$	1.70×10^{-11}	[c]
18	$CF_3OC(O)OONO_2 \rightarrow CF_3OC(O)OO + NO_2$	3.35×10^{-4}	[13]
19	$CF_3OC(O)OO + NO \rightarrow CF_3OC(O)O + NO_2$	2.60×10^{-11}	[d]
20	$CF_3OC(O)OO + Cl \rightarrow CF_3OC(O)O + ClO$	4.20×10^{-11}	Assumed similar to react 12
21	$2CF_3OC(O)OO \rightarrow 2CF_3OC(O)O + O_2$	9.20×10^{-12}	[32]
22	$CF_3OC(O)OO + CF_3OO \rightarrow CF_3OC(O)O + O_2 + CF_3O$	9.20×10^{-12}	Assumed similar to react 21
23	$CF_3OC(O)OO + CF_3CF_2OO \rightarrow CF_3OC(O)O + O_2 + CF_3CF_2O$	9.20×10^{-12}	Assumed similar to react 21
24	$CF_3OC(O)O \rightarrow CF_3O + CO_2$	4.00×10^{1}	[13]
25	$CF_3OO + NO_2 \rightarrow CF_3OONO_2$	6.00×10^{-12}	[30]
26	$CF_3OO + CF_3CF_2OO \rightarrow CF_3O + O_2 + CF_3CF_2O$	2.26×10^{-12}	Assumed similar to react 11
27	$CF_3OONO_2 \rightarrow CF_3OO + NO_2$	5.92×10^{-2}	[18]
28	$CF_3O + wall \rightarrow CF_2O$	2.00×10^{2}	This work
29	$Cl + Cl \rightarrow Cl_2$	1.00×10^{-13}	[33]
30	$CF_3O + NO_2 \rightarrow CF_2O + FNO$	3.20×10^{-12}	[28]
31	$Cl + CO \rightarrow ClCO$	2.00×10^{-15}	[34]
32	$ClCO \rightarrow Cl + CO$	3.00×10^{5}	[35]
33	$ClCO + O_2 \rightarrow ClC(O)OO$	4.51×10^{-13}	[36]
34	$2ClC(O)OO \rightarrow 2ClCOO + O_2$	5.00×10^{-12}	[e]
35	$ClCOO \rightarrow Cl + CO_2$	4.00×10^{-4}	[f]
36	$NO_2 \rightarrow NO$	1.08×10^{-5}	[g]

[a] First-order reactions, in s^{-1}; second-order reactions, in cm^3 $molecule^{-1}$ s^{-1}.
[b] Assumed similar to $CF_3CF_2CF_2OO$ [10].
[c] Assumed similar to CF_3CO [31,11].
[d] Assumed similar to $CF_3C(O)OO + NO$ [32].
[e] Assumed similar to $FC(O)OO$ [37].
[f] Fixed to give the observed CO_2 concentration.
[g] Calculated from UV absorption cross-sections of NO_2 and photon flux.

3.2. Isolation and recognition of $CF_3CF_2OONO_2$. Infrared absorption cross-sections

Fig. 4 shows the infrared spectra obtained during the synthesis of $CF_3CF_2OONO_2$ when mixtures of $CF_3CF_2C(O)Cl$ (2.0 mbar)/NO_2 (1.0 mbar)/O_2 (1000 mbar) at 13 °C were photolyzed. The progress of peroxynitrate formation was monitored every 30 min and the photolysis was stopped before NO_2 disappearance in order to ensure that the formation of $CF_3CF_2OONO_2$ is favored. As it can be seen, peaks at 1764 and 790 cm^{-1}, corresponding to the peroxynitrate, increase as time elapses. The formation of CF_2O (1959 and 774 cm^{-1}) could also be observed.

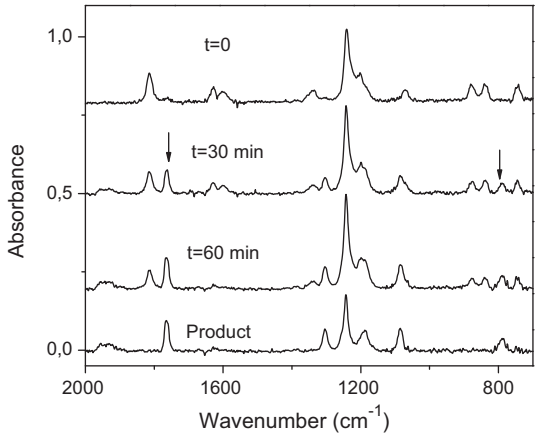

Fig. 4. IR spectra in the photolysis of mixtures of $CF_3CF_2C(O)Cl/NO_2/O_2$ at 13 °C. Arrows show the peaks corresponding to $CF_3CF_2OONO_2$ formed. Last trace shows the photolysis products.

The infrared bands (cm^{-1}), the corresponding absorbance cross-sections (σ, cm^2 $molecule^{-1}$), and the tentative assignments are 790 (1.11 ± 0.08) NO_2 def. δNO_2, 1085 (2.2 ± 0.2) ν_{as}(C—F), 1188 (1.57 ± 0.08) ν_{as} (CF_3), 1244 (4.8 ± 0.5) ν_{as} (CF_3), 1304 (1.63 ± 0.09) ν_s (NO_2), 1764 (2.54 ± 0.09) ν_{as} (NO_2), in good agreement with the bands and the assignments for the other fluorinated peroxynitrates of similar structure e.g. CF_3OONO_2 [14], $CF_3C(O)OONO_2$ [15], and $CF_3CF_2C(O)OONO_2$ [16].

3.3. Thermal decomposition

The pentafluoroethyl peroxynitrate exists in equilibrium with NO_2 and $CF_3CF_2OO^{\bullet}$ radicals

$$CF_3CF_2OONO_2 \rightarrow CF_3CF_2OO^{\bullet} + NO_2 \quad (3a)$$

$$CF_3CF_2OO^{\bullet} + NO_2 \rightarrow CF_3CF_2OONO_2 \quad (3b)$$

In order to measure the rate constant for decomposition, the presence of a radical scavenger is needed. NO was added since it

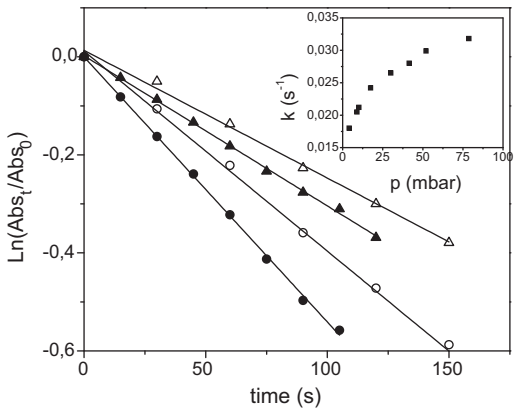

Fig. 5. First-order decay plot for the thermal decomposition of $CF_3CF_2OONO_2$. Open and solid symbols correspond to total pressures of 9.0 and 250 mbar, while triangles and circles correspond to 282.9 and 287.5 K, respectively. The insert shows the dependence of the rate constant with pressure for pressures under 100 mbar.

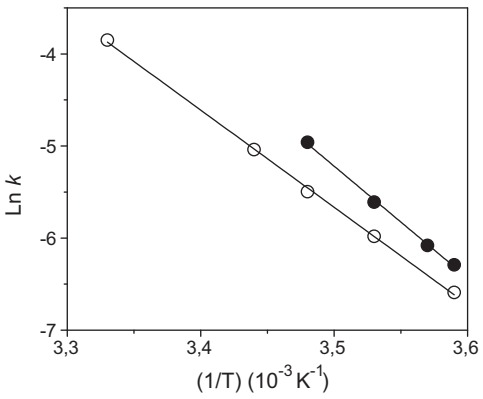

Fig. 6. Arrhenius plot for the thermal decomposition of $CF_3CF_2OONO_2$ at 9.0 and 250 mbar of total pressure.

efficiently removes the $CF_3CF_2OO^\bullet$ radicals, leading to the formation of CF_2O, CF_3NO, and NO_2 from the following reactions:

$$CF_3CF_2OO^\bullet + NO \rightarrow CF_3CF_2O^\bullet + NO_2 \quad (4)$$

$$CF_3CF_2O^\bullet \rightarrow CF_3^\bullet + CF_2O \quad (5)$$

$$CF_3^\bullet + NO \rightarrow CF_3NO \quad (6)$$

Fig. 5 shows the first-order plot for the disappearance of $CF_3CF_2OONO_2$ measured following the band at 1764 cm^{-1} for two different pressures (9.0 and 250 mbar) and two selected temperatures (282.9 and 287.4 K). As it can be seen, the rate constant depends on both parameters. All the rate constants measured are listed in column 3 of Table 2. These values were corrected considering that, as time elapses, the NO added leads to an increase in NO_2 formation, slightly shifting the equilibrium toward the formation of $CF_3CF_2OONO_2$ via reaction (3b). The equation used to correct the rate constant has been reported elsewhere [17]

$$k_1 = k_{obs}\left(1 + \frac{k_{-2}[NO_2]}{k_3[NO]}\right)$$

where k_{obs} corresponds to the uncorrected experimental rate of disappearance of $CF_3CF_2OONO_2$. The ratio $k_{-2}/k_3 = 0.64$ was determined from Table 1. The corrected values are listed in column 4. Note that at room temperature, the rate constant was measured only at 9.0 mbar since the thermal decomposition is very fast and cannot be experimentally measured at a higher pressure.

After correcting the rate constants, we plotted the pressure dependence of k_2 at 300.3 K as the inset of Fig. 5. Total pressure was reached adding the necessary amount of N_2. The trend for the pressure dependence observed for $CF_3CF_2OONO_2$ is similar to that determined for CF_3OONO_2 by Mayer-Figge et al. [18] for pressures ranging between 4.0 and 1013 mbar.

Table 2
Corrected and uncorrected rate constants for thermal decomposition of $CF_3CF_2OONO_2$ at 9.0 and 250 mbar total pressure, at different temperatures.

T (K)	Total pressure (mbar)	$k_{uncorrected}$ (10^{-3} s^{-1})	k_{corr} (10^{-3} s^{-1})
278.7	9.0	1.33	1.37 ± 0.07
283.1	9.0	2.41	2.5 ± 0.1
287.7	9.0	3.79	4.1 ± 0.2
290.9	9.0	6.09	6.5 ± 0.2
300.3	9.0	17.0	21.2 ± 0.7
278.6	250	1.50	1.86 ± 0.08
279.8	250	1.79	2.3 ± 0.1
283.1	250	3.06	3.7 ± 0.1
287.7	250	5.4	7.0 ± 0.2

The temperature dependence of the first-order rate constant, k_2, is shown in Fig. 6. The activation energy (E_a) and pre-exponential factor obtained at 9.0 and 250 mbar were: $E_a = 87.7$ kJ/mol, $A = 3.8 \times 10^{13}$; and $E_a = 96.7$ kJ/mol, $A = 2.37 \times 10^{15}$, respectively. E_a decreases with the decrease in total pressure, in agreement with unimolecular reaction rate theories. This result is in accordance with that measured for CF_3OONO_2 [18]. With this in mind and the values found for CF_3OONO_2 ($E_a = 90.8$ kJ/mol, $A = 1.05 \times 10^{14}$ at 10.6 mbar; $E_a = 94.2$ kJ/mol $A = 9.1 \times 10^{14}$ at 104.3 mbar; and $E_a = 97.7$ kJ/mol, $A = 5.7 \times 10^{15}$ at 1013 mbar [18]) it is possible to suggest that the value for E_a at pressures close to one atmosphere could be around 98 kJ/mol.

The rate constant $k_2 = 2.88 \times 10^{-2}$ s^{-1} can be compared with 4.28×10^{-2} s^{-1}, 3.92 s^{-1} and 6.12 s^{-1} obtained for CF_3OONO_2 [18], CH_3OONO_2, and $CH_3CH_2OONO_2$ [19], respectively, and the comparison indicates that fluorinated alkyl peroxynitrates are more stable than their non-fluorinated analogs. The comparison also suggests that the rate constant decreases with the length of the alkyl group.

Fig. 7 shows the thermal lifetime profile of $CF_3CF_2OONO_2$, CF_3OONO_2, $CH_3C(O)OONO_2$ (PAN), and $CH_3CH_2C(O)OONO_2$ (PPN). Thermal lifetimes for $CF_3CF_2OONO_2$ have been calculated from the kinetic parameters obtained in this work, and for CF_3OONO_2, PAN, and PPN using the Arrhenius parameters informed in references [18,20,21]. As it can be seen, $CF_3CF_2OONO_2$ lifetime is similar to that obtained for CF_3OONO_2, and shorter than those calculated for PAN and PPN.

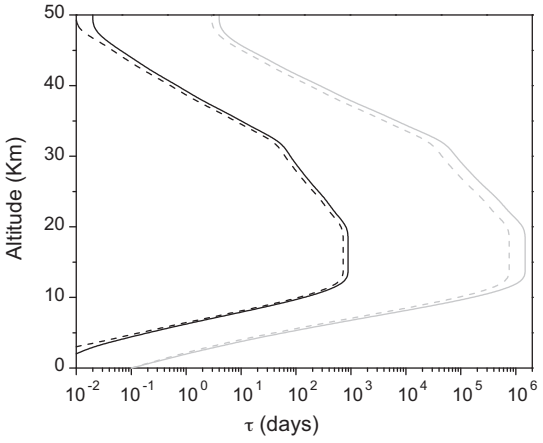

Fig. 7. Atmospheric thermal lifetimes for several peroxynitrates. $CF_3CF_2OONO_2$ (black solid line), CF_3OONO_2 (black dashed line) [18], PAN (gray dashed line) [22], PPN (gray solid line) [23].

Thermal lifetimes for pentafluoroethyl peroxynitrate are longer than one day at altitudes higher than 6 km, and they reach values higher than 100 days at altitudes between 10 and 25 km, precisely where solar radiation (short wavelengths) is sufficient to photolyze $CF_3CF_2C(O)Cl$, leading to $CF_3CF_2OONO_2$ formation. Consequently, this new peroxynitrate could act as a reservoir species of NO_2 and $CF_3CF_2OO^{\bullet}$ radicals in the stratosphere.

4. Conclusions

The study of the photochemistry of $CF_3CF_2C(O)Cl$ in the presence of NO_2 and O_2 shows that the products formed depend on NO_2 concentration, i.e. on the level of NO_x present in different environments. The goal of this work was the identification of $CF_3CF_2OONO_2$, a new peroxynitrate formed by the photooxidation of $CF_3CF_2C(O)Cl$, which in turn is produced by the atmospheric degradation of HCFC-225ca ($CF_3CF_2CHCl_2$).

Acknowledgments

Financial support from SECYT-Universidad Nacional de Córdoba, ANPCyT, and CONICET is gratefully acknowledged. AB acknowledges the fellowship she holds from CONICET.

References

[1] WMO (World Meteorological Organization), Scientific Assessment of Ozone Depletion: 1991, Global Ozone Research and Monitoring Project, Report No. 25, Geneva, Switzerland, 1992.
[2] F.S. Rowland, M.J. Molina, Rev. Geophys. Space Phys. 13 (1975) 1.
[3] T.J. Wallington, W.F. Schneider, D.R. Worsnop, O.J. Nielsen, J. Sehested, W. DeBruyn, J.A. Shorter, Environ. Sci. Technol. 28 (1994) 320.
[4] E.C. Tuazón, R. Atkinson, J. Atmos. Chem. 17 (1993) 179.
[5] F.E. Malanca, M. Burgos Paci, G.A. Argüello, J. Photochem. Photobiol. 150 (2002) 1.
[6] F.E. Malanca, K.L. Bierbrauer, M.S. Chiappero, G.A. Argüello, J. Photochem. Photobiol. 149 (2002) 9.
[7] S.A. Cariati, D.E. Weibel, E.H. Staricco, J. Photochem. Photobiol. A 123 (1999) 1.
[8] F.E. Malanca, G.A. Argüello, E.H. Staricco, J. Photochem. Photobiol. A 103 (1997) 19.
[9] J.C. Ianni, KINTECUS V 4.0.0.
[10] A.M.B. Giessing, A. Feilberg, T.E. Mogelberg, J. Sehested, M. Bilde, T.J. Wallington, O.J. Nielsen, J. Phys. Chem. 100 (1996) 6572.
[11] T.J. Wallington, J. Sehested, O.J. Nielsen, Chem. Phys. Lett. 226 (1994) 563.
[12] S.P. Sander, R.R. Friedl, D.M. Golden, M.J. Kurylo, G.K. Moortgat, H. Keller-Rudek, P.H. Wine, A.R. Ravishankara, C.E. Kolb, M.J. Molina, B.J. Finlayson-Pitts, R.E. Huie, V.L. Orkin, Chemical kinetics and photochemical data for use in atmospheric studies, Evaluation No. 15, JPL Publication 06-2.
[13] M.D. Manetti, F.E. Malanca, G.A. Argüello, Int. J. Chem. Kinet. 40 (2008) 831.
[14] R. Kopitzky, H. Willner, H.G. Mack, A. Pfeiffer, H. Oberhammer, Inorg. Chem. 37 (1998) 6208.
[15] R. Kopitzky, M. Beuleke, G. Balzer, H. Willner, Inorg. Chem. 36 (1997) 1994.
[16] M.P. Sulbaek Andersen, M.D. Hurley, T.J. Wallington, J.C. Ball, J.W. Martin, D.A. Ellis, S.A. Mabury, O.J. Nielsen, Chem. Phys. Lett. 379 (2003) 28.
[17] L.K. Christensen, T.J. Wallington, A. Guschin, M.D. Hurley, J. Phys. Chem. A 103 (1999) 4202.
[18] A. Mayer-Figge, F. Zabel, K.H. Becker, J. Phys. Chem. 100 (1996) 6587.
[19] R. Atkinson, D.L. Baulch, R.A. Cox, R.F. Hampson, J.A. Kerr Jr., M.J. Rossi, J.J. Troe, J. Phys. Chem. Ref. Data 26 (1997) 521.
[20] I. Bridier, F. Caralp, H. Loirat, R. Lesclaux, B. Veyret, K.H. Becker, A. Reimer, F. Zabel, J. Phys. Chem. 95 (1991) 3594.
[21] F. Kirchner, A. Mayer-Figge, F. Zabel, K.H. Becker, Int. J. Chem. Kinet. 31 (1999) 127.
[22] R. Atkinson, D.L. Baulch, R.A. Cox, R.F. Hampson Jr., J.A. Kerr, J. Troe, J. Phys. Chem. Ref. Data 18 (1989) 881.
[23] R.V. Olkhov, I.W.M. Smith, Phys. Chem. Chem. Phys. 5 (2003) 3436.
[24] L. Florent, D.R. Burgess Jr., M.T. Rayez, J.P. Sawerysyn, Phys. Chem. Chem. Phys. 1 (1999) 5087.
[25] H. Somnitz, R. Zellner, Phys. Chem. Chem. Phys. 3 (2001) 2352.
[26] F. Caralp, R. Lesclaux, A.M. Dognon, Chem. Phys. Lett. 129 (1986) 433.
[27] J. Sehested, T. Mogelberg, K. Fagerstrom, G. Mahmoud, T.J. Wallington, Int. J. Chem. Kinet. 29 (1997) 673.
[28] F. Caralp, M.T. Rayez, W. Forst, C. Bourbon, M. Brioukov, P. Devolder, J. Chem. Soc. Faraday Trans. 93 (1997) 3751.
[29] R. Atkinson, D.L. Baulch, R.A. Cox, J.N. Crowley, R.F. Hampson Jr., J.A. Kerr, M.J. Rossi, J. Troe, Summary of Evaluated Kinetic and Photochemical Data for Atmospheric Chemistry, IUPAC Subcommittee on Gas Kinetic Data Evaluation for Atmospheric Chemistry Web Version December, 2001, 1.
[30] W.B. DeMore, S.P. Sander, D.M. Golden, R.F. Hampson, M.J. Kurylo, C.J. Howard, A.R. Ravishankara, C.E. Kolb, M.J. Molina, Chemical kinetics and photochemical data for use in stratospheric modeling, Evaluation No. 12, JPL Publication 97-4, 1997, 1.
[31] T.J. Wallington, M.D. Hurley, O.J. Nielsen, J. Sehested, J. Phys. Chem. 98 (1994) 5686.
[32] M.M. Maricq, J.J. Szente, G.A. Khitrov, J.S. Francisco, J. Phys. Chem. 100 (1996) 4514.
[33] D.L. Baulch, J. Duxbury, S.J. Grant, D.C. Montague, J. Phys. Chem. Ref. Data 10 (1981) 1.
[34] R. Atkinson, D.L. Baulch, R.A. Cox, J.N. Crowley, R.F. Hampson, R.G. Hynes, M.E. Jenkin, M.J. Rossi, J. Troe, J. Atmos. Chem. Phys. 7 (2007) 981.
[35] W.B. DeMore, S.P. Sander, D.M. Golden, R.F. Hampson, M.J. Kurylo, C.J. Howard, A.R. Ravishankara, C.E. Kolb, M.J. Molina, Chemical kinetics and photochemical data for use in stratospheric modeling. Evaluation No. 10, JPL Publication 92-20, 1.
[36] A.D. Hewitt, K.M. Brahan, G.D. Boone, S.A. Hewitt, Int. J. Chem. Kinet. 28 (1996) 763.
[37] T.J. Wallington, T. Ellermann, O.J. Nielsen, J. Sehested, J. Phys. Chem. 98 (1994) 2346.